

Electrochemical Investigation and Modeling of Cathodic Reactions on Iron Sulfides in Acidic Solutions

Payman Sharifi Abdar, Bruce Brown, Srdjan Nestic
Institute for Corrosion and Multiphase Technology, Ohio University
342 W State Street
Athens, Ohio, 45701
USA

ABSTRACT

With an increasing number of sour oil and gas fields in the world, mitigation of production related failures due to H₂S corrosion is a key challenge. In H₂S environments, the corrosion product layer could include different types of iron sulfides with various electrical and physiochemical properties. One of the main characteristics of iron sulfides is their semiconductive nature which could enhance the galvanic coupling between steel and this type of corrosion product layer. On that account, galvanic coupling between steel and iron sulfides is considered as the main culprit related to the higher risk of localized corrosion in H₂S environments. However, the mechanism of galvanic coupling between steel and iron sulfides are still unclear as the nature of iron sulfides transformation and their electrochemical behavior have not been fully understood yet. The objective of this study is to investigate and model the electrochemical behavior of iron sulfides by specifically focusing on their cathodic characteristics in acidic solutions. Pyrite and pyrrhotite were used as the iron sulfides for these tests since they have been found when localized corrosion of steel was observed in sour pipeline conditions in the field. A rotating disk electrode (RDE) has been utilized for investigation of cathodic reactions occurring on the surface of pyrite, pyrrhotite, and X65 steel. Experiments have been performed in several pH values as well as different rotational speeds in order to characterize the nature of cathodic reactions. In addition, a mathematical model was developed to predict the cathodic current of iron sulfides, and then the results were compared with the experimental data.

Key words: Galvanic corrosion, Pitting, Hydrogen sulfide, Electrochemistry, Corrosion products

INTRODUCTION

H₂S corrosion, also known as sour corrosion, is a very serious type of metal degradation in oil and gas transmission pipelines. When H₂S is present in an operating pipeline, localized corrosion is the type of attack which contributes to the most failures in oilfields, consequently, its impact on the economics of oil and gas production is indisputable. Therefore, mitigation of this type of corrosion could prevent such failures and significantly enhance asset integrity while reducing maintenance costs as well as eliminating

environmental damage. The unpredictability of pitting and localized corrosion in sour media is a complicated challenge in this area as factors such as the nature of corrosion products, the formation of inhomogeneous corrosion product layers, and the contribution of galvanic coupling play a role in this type of corrosion^{1,2}.

Galvanic coupling between iron sulfides and mild steel is thought to be an important mechanism leading to localized corrosion in H₂S environments. Research done by Ning³ proved that galvanic coupling between pyrite and steel caused severe localized corrosion. In a set of experiments designed to separate the galvanic effect from the chemical effects, pyrite particles and a thin nylon mesh were used. Pyrite particles were placed directly on a steel surface at 25 °C, pH₂S of 0.1 bar, 1 wt.% NaCl and pH 4 which resulted in severe localized corrosion. In the same conditions, when a 60 μm nylon mesh was placed between the pyrite particles and the steel surface, no localized attack was observed when the pyrite was not in direct contact with the metal surface. This experiment showed that the localized corrosion process has an electrochemical nature⁴ because the initiation of pitting corrosion was dependent upon physical contact for transfer of electrons and not just close physical proximity for chemical reactions to occur.

The galvanic coupling between steel and iron sulfides and the effect of experimental parameters including iron sulfide type, cathode to anode surface area ratio, and salt concentration, have been systematically investigated by the authors in a previous study⁴. However, the prediction of galvanic current is not achievable without understanding the electrochemical characteristics of iron sulfides. Since iron sulfides act as the cathode in a steel-iron sulfide couple, the cathodic current of iron sulfides should be known to predict the accurate galvanic current. Very few studies have investigated the electrochemical reactions, specifically cathodic reactions, occurring on iron sulfides. The only systematic research to date was done by Navabzadeh et al.⁵, which investigated the cathodic behavior of X65 steel, pyrite, and pyrrhotite in various acidic solutions at different pH values using a rotating disk electrode (RDE) apparatus. Therefore, this study aims to investigate the cathodic behavior of iron sulfides in various experimental conditions in strong acid solutions using the same type RDE system. Strong acid solutions were selected because the presence of H₂S has been observed to enhance the cathodic current of steel and iron sulfides by contributing to limiting current through the buffering effect^{5,6}, but a significant chemical interaction between H₂S and iron sulfides has not been observed⁵. In addition, a mathematical model was developed for modeling the cathodic current on iron sulfides.

EXPERIMENTAL PROCEDURE

In this study, a rotating disk electrode (RDE) has been used which is a very useful system for electrochemical measurements since its hydrodynamics and mass transfer have been well defined in the literature⁷. Two types of iron sulfides (pyrite and pyrrhotite) have been used as well as API 5L X65 steel (composition shown in Table 1) for comparison with the iron sulfide results. Mineral pyrite and pyrrhotite were purchased from Ward's Science. For purity analysis, these minerals were powdered by pestle and mortar, then characterized by XRD measurement using Cu K α radiation as shown in Figure 1. Very high purity was observed for the pyrite sample when compared to the reference pattern ICDD# 00-0042-1340. The purity of the pyrrhotite sample was also verified according to the reference pattern ICSD# 01-079-5969, however, minor impurities are present. These mineral iron sulfides were cut to the right shape and embedded in epoxy fitted in the rotating disk electrode system. In addition, a silver conductive paste was placed on the back of the mineral samples to improve the conductivity for the gold spring contact inside the RDE holder.

Table 1
Chemical composition of API 5L X65 carbon steel (in wt.%)

Cr	Cu	Mn	Mo	C	Co	Ni	Si	Ti	As
0.15	0.14	1.51	0.16	0.05	0.012	0.38	0.25	0.01	0.015
P	S	Al	Sn	Sb	V	Zr	Nb	Fe	
0.004	0.001	0.033	0.035	0.012	0.04	0.004	0.03	balance	

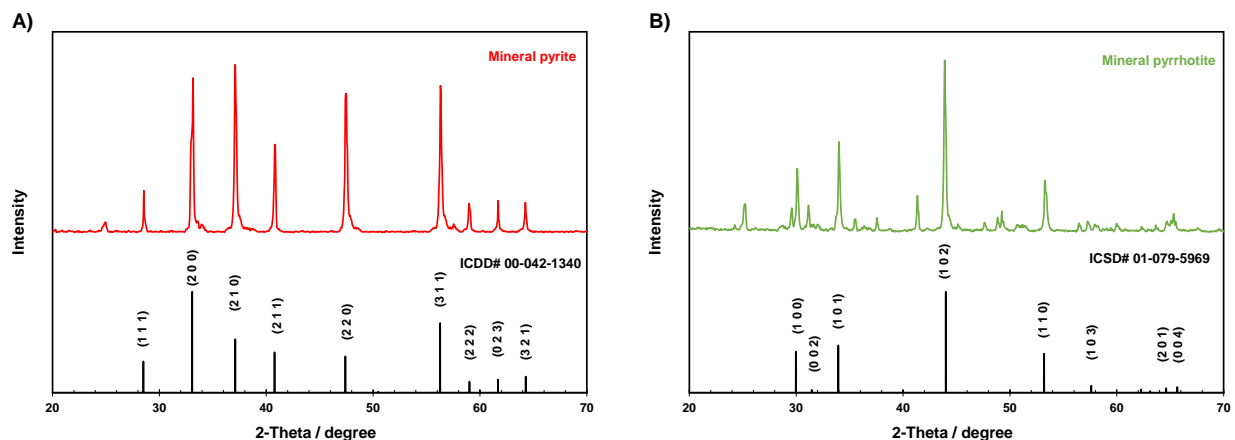
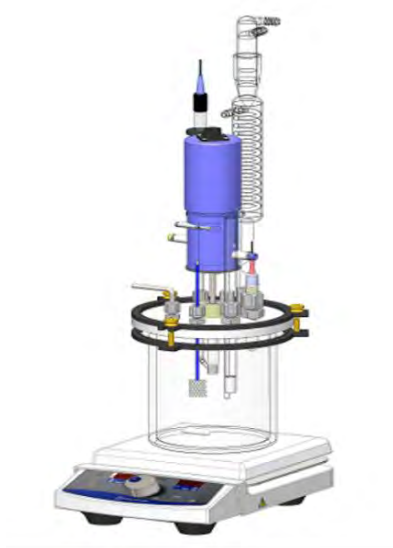


Figure 1: XRD analysis of mineral iron sulfide samples. A) pyrite, B) pyrrhotite

A platinum mesh counter electrode (CE) and a saturated Ag/AgCl reference electrode (RE) were used. The experiments were performed in strong acid solutions with 1 wt.% NaCl. In order to characterize the nature of cathodic reactions, the experiments were done in various pH (3, 4, and 5) and rotational speeds (100 and 1000 rpm). Electrochemical impedance spectroscopy was utilized for the measurement and compensation of solution resistance. Cathodic polarizations were performed with the scan rate of 0.5 mV/s after running open circuit potential measurements for about 30 minutes using a Gamry Reference 600 potentiostat. An overview of the experimental setup and test matrix are shown in Figure 2.



Parameter	Conditions
Material	X65, Pyrite, Pyrrhotite
Steel Size	5 mm \varnothing
pH	3.0, 4.0, 5.0 \pm 0.1
rpm	100, 1000
Temperature	25°C
Electrolyte	1 wt.% NaCl
Sparge Gas	N ₂
Electrochemical Techniques	Cathodic polarization 0.5 mV/s EIS for solution resistance

Figure 2: Overview of the RDE experimental setup and test matrix.

RESULTS

Cathodic Current on Steel and Iron Sulfides

The cathodic polarizations of steel and pyrite in pH values of 3 and 4, at two rotational speeds are shown in Figure 3. As seen in the figure, two major reduction reactions occur on the surface of steel in strong acid solutions: hydrogen ion reduction (at more positive potentials close the open circuit potential, OCP) and water reduction (at more negative potentials). Similar reduction reactions can be found on the surface of pyrite, in addition, a third reduction reaction was observed to occur at even more positive potentials which was not observed for steel. These three reduction reactions will be discussed in the following in order to gain an understanding of cathodic characteristics of pyrite.

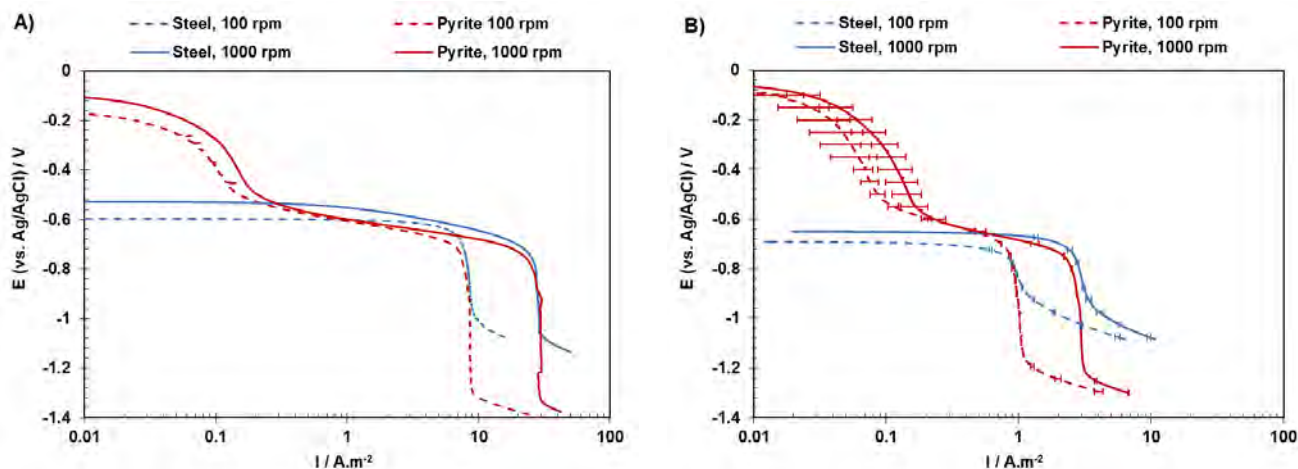


Figure 3: Comparison of cathodic current densities on the surface of steel and pyrite for 100 and 1000 rpm at A) pH 3, and B) pH 4 (RDE, 25°C, 1 wt.% NaCl, 1 bar, sparged with N₂).

The limiting current value can be verified by comparing to the theoretical limiting current density developed for rotating disk electrode system using Levich equation as shown below⁷.

$$i_L = 0.62nFD^{(2/3)}\omega^{(1/2)}\nu^{(-1/6)}C_b \quad (1)$$

where n is the number of electrons transferred in the reaction, F is the Faraday constant, D is the diffusivity, ω is the rotational speed in rad/s, ν is the kinematic viscosity of solution, and C_b is the concentration of species [H⁺] in the bulk solution. The Levich equation depends on two experimental parameters, which are the concentration of ions, or pH, and rotational speed. The limiting current should be associated with the hydrogen reduction reaction, as influenced by the bulk concentration of species, independent of the type of material.

As can be observed from Figure 3, the limiting current density on the surface of pyrite fits to that obtained on steel surface at different pH values for both rotational speeds. Furthermore, the measured value of limiting current densities in all conditions agree well with the theoretical calculated values using Levich equation. These results clearly confirm the occurrence of hydrogen reduction reaction on pyrite surface at potentials around the open circuit potential of steel. The charge transfer part (~120 mV/dec Tafel slope) of this reaction does seem to be detectable for steel at 1000 rpm and pH 3, but not at the other tested conditions. However, the charge transfer part can be clearly identified for pyrite in all four cathodic sweeps in Figure 3. The charge transfer current density does not change with rotational speed at a constant pH which implies that it only depends on the concentration of H⁺. With regards to the water reduction reaction occurring at very low potentials, the results show that the onset potential of this reaction on the surface

© 2023 Association for Materials Protection and Performance (AMPP). All rights reserved. No part of this publication may be reproduced, stored in a retrieval system, or transmitted, in any form or by any means (electronic, mechanical, photocopying, recording, or otherwise) without the prior written permission of AMPP.

Positions and opinions advanced in this work are those of the author(s) and not necessarily those of AMPP. Responsibility for the content of the work lies solely with the author(s).

of pyrite is more negative than on the surface of steel. This observation signifies that the water reduction reaction was retarded at the surface pyrite.

After reviewing the similarities for the limiting current of the hydrogen reduction reaction and the differences for the water reduction reaction, a review is also needed for the reduction reaction which occurs on the pyrite surface at high potentials. No direct research has been found related to the cathodic polarization of pyrite, but some cyclic voltammetry studies of pyrite⁸⁹ in acidic solutions proposed that the reaction could be the reduction of pyrite to FeS according to Reaction (2).



Studying the effect of pH and rotational speed could be very helpful in understanding the nature of this reaction. However, the change of pH does not affect the current density of this reaction as represented in Figure 3. In other words, increasing the concentration of the H⁺ ion did not directly influence the reaction, which means that either the H⁺ ion does not participate in this unknown reaction, or it is not a limiting factor for the reaction. The change of rotational speeds showed a slight effect, but much lower than is seen for the limiting current of hydrogen reduction reaction, indicating that this reaction might not be sensitive to the effects of mass transfer.

The same experiments and evaluation were performed for the characterization of the cathodic reactions on pyrrhotite. Figure 4 shows the cathodic polarization of pyrrhotite and steel at two pH values and two rotational speeds. Analogous to the pyrite case, three cathodic reactions can be distinguished at the surface of pyrrhotite, although it is less clear at pH 4. The water reduction at more negative potentials was retarded on the surface of pyrrhotite compared with steel, showing similar behavior between pyrrhotite and pyrite regarding water reduction.

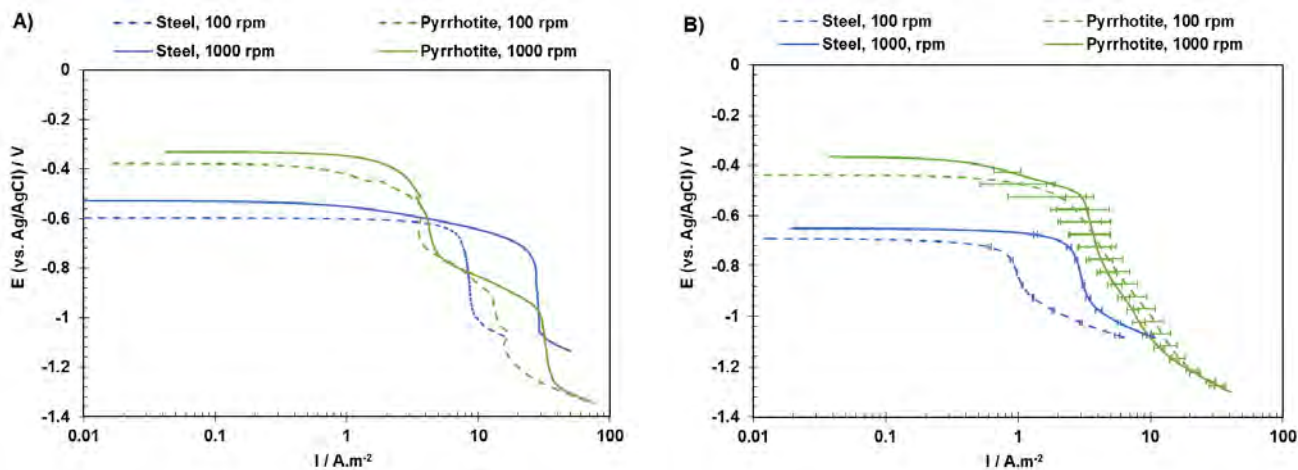


Figure 4: Comparison of cathodic current densities on the surface of steel and pyrrhotite for 100 and 1000 rpm at A) pH 3 and B) pH 4 (RDE, 25°C, 1 wt.% NaCl, 1 bar, sparged with N₂).

For pyrrhotite, the Tafel region of the hydrogen reduction reaction can be observed only for the cathodic sweeps at pH 3. Also, at pH 3, changing the rotational speed influenced the limiting current density of the hydrogen reduction reaction on pyrrhotite. The limiting current density on the surface of pyrrhotite is equal to the one obtained on the surface of steel at 1000 rpm and follows the Levich equation which confirms the presence of the hydrogen reduction reaction. At 100 rpm, the limiting current density of pyrrhotite is slightly higher than steel which is due to the effect of high current density associated with pyrrhotite reduction reaction. However, at pH 4, the limiting current density is masked due the presence of another reaction with a higher current density. This reaction was also seen at pH 3 and sits “above” the hydrogen reduction reaction, i.e. at potentials more positive than the open circuit potential of steel. It seems that the current density of this reaction does not alter with respect to pH. Therefore, when its current density

is lower than the limiting current density of hydrogen reduction at pH 3, it dominates this limiting current density at pH 4. Although few studies investigated the nature of this reaction, it is mostly associated with the reduction of pyrrhotite to troilite or FeS according to Reactions (3) and (4)⁸¹⁰.

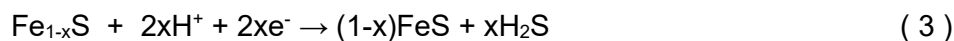


Figure 5 compares the cathodic currents on the surface of steel, pyrite, and pyrrhotite at pH 3, and 4. At pH 3, hydrogen reduction reaction including both mass transfer limiting as well as charge transfer regions are noticeable on the surface of both pyrite and pyrrhotite. The current density associated with pyrrhotite reduction is about an order of magnitude larger than that associated with pyrite reduction. The same observation can be seen at pH 4 regarding the significant difference in the current density magnitude between pyrite and pyrrhotite behaviors. However, the hydrogen reduction reaction is not apparent at this condition due to the very high current density on the pyrrhotite surface. This high current density of pyrrhotite reduction could be due to the physicochemical structure of this iron sulfide. Although pyrite is the most stable polymorph of iron sulfides, pyrrhotite can be further reduced to more stable phases such as troilite which results in the high electroactivity of this material.

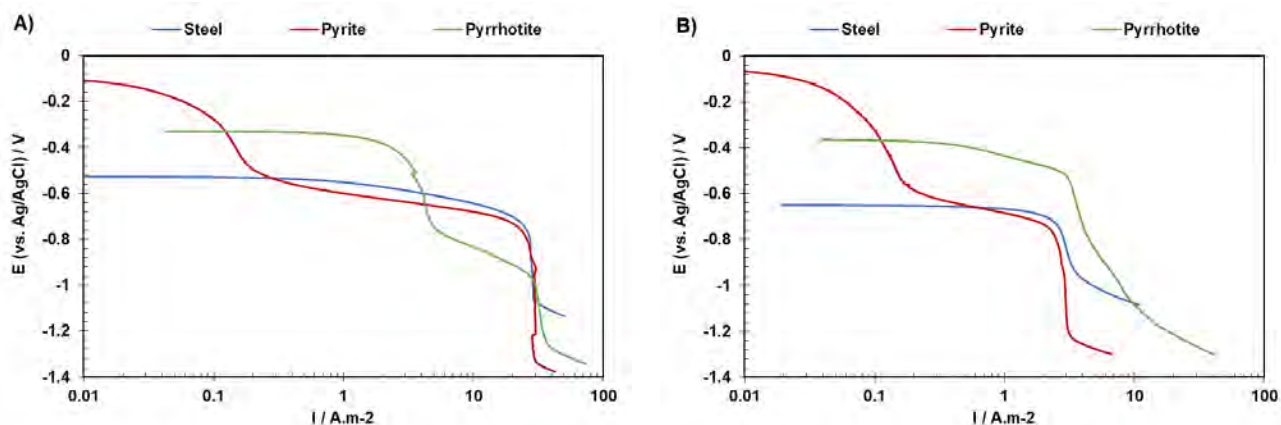


Figure 5: Comparison of cathodic current densities on various surfaces at 1000 rpm at A) pH 3 and B) pH 4.

Mathematical Modeling

The total current for the hydrogen reduction reaction consists of both charge transfer current and mass transfer limiting current. The limiting current can be found using the Levich equation as shown by Equation (5). The charge transfer current can be calculated via Equation (6) in which the exchange current density can be found from Equation (7). Therefore, the total cathodic current for the hydrogen reduction reaction can be calculated using Equation (8). As water is always available on the surface of electrode, the current for the water reduction reaction is a sole charge transfer current which can be found using Tafel Equation (9) with exchange current density calculated using Equation (10). In order to calculate the cathodic current of the reduction reaction on the surface of iron sulfides, these currents were treated as a limiting current density with constant current densities found from experimental results. This is a first simple approach that was used in this study which is expected to be improved in future research. Also, as these high potential currents are expected to be minimally associated with the coupled potential region, this assumption is reasonable and should not significantly affect the modeling results. All the equations are shown in Table 2.

Table 2
Equations used for modeling the cathodic current.

$i_{H^+,lim} = 0.62FD^{2/3}v^{(-\frac{1}{6})}\omega^{1/2}c_{H^+}$	(5)
$i_{H^+,ct} = i_{0,H^+} \times 10^{-\frac{\eta}{b_c}}$	(6)
$i_{0,H^+} = i_{0,H^+}^{ref} \left(\frac{c_{H^+}}{c_{H^+,ref}} \right)^{0.5} \times e^{-\frac{\Delta H}{R} \left(\frac{1}{T} - \frac{1}{T_{ref}} \right)}$	(7)
$\frac{1}{i_{H^+}} = \frac{1}{i_{H^+,ct}} + \frac{1}{i_{H^+,lim}}$	(8)
$i_{H_2O} = i_{0,H_2O} \times 10^{-\frac{\eta}{b_c}}$	(9)
$i_{0,H_2O} = i_{0,H_2O}^{ref} \left(\frac{c_{H^+}}{c_{H^+,ref}} \right)^{-0.5} \times e^{-\frac{\Delta H}{R} \left(\frac{1}{T} - \frac{1}{T_{ref}} \right)}$	(10)
$i_{pyrite\ reduction, lim} = constant$	(11)
$i_{pyrrhotite\ reduction, lim} = constant$	(12)

For modeling the current on the surface of steel, all the constants and parameters used in the equation were derived from the FREECORP manual available freely at Institute for Corrosion and Multiphase Technology (ICMT) website¹¹. All the values for parameters used in the calculation of cathodic current on iron sulfides were derived from experimental results. All values used for modeling are listed in Table 3.

Table 3.
Parameter values used in equations defined in Table 2

Parameter	Steel	Pyrite	Pyrrhotite
$i_{0,H^+}^{ref} \left(\frac{A}{m^2} \right)$	3×10^{-2}	1.75×10^{-4}	10^{-4}
$c_{H^+,ref} \text{ (M)}$	10^{-4}	10^{-4}	10^{-4}
$\Delta H \left(\frac{kJ}{mol} \right)$	30	30	30
$b_{c,H^+} \left(\frac{V}{dec} \right)$	0.12	0.09	0.12
$T_{ref} \text{ (}^\circ\text{C)}$	20	20	20
$E_{rev,H^+} \text{ (V)}$	$-0.059 \times \text{pH}$	$-0.034 \times \text{pH}$	$-0.09 \times \text{pH}$
$i_{0,H_2O}^{ref} \left(\frac{A}{m^2} \right)$	2×10^{-5}	2×10^{-5}	10^{-4}
$b_{c,H_2O} \left(\frac{V}{dec} \right)$	0.12	0.12	0.16
$E_{rev,H_2O} \text{ (V)}$	$-0.059 \times \text{pH}$	$-0.059 \times \text{pH}$	$-0.059 \times \text{pH}$
$i_{iron\ sulfide, lim} \left(\frac{A}{m^2} \right)$	-	0.13 for 1000 rpm 0.1 for 100 rpm	4

Model Verification

In order to validate the model developed for the cathodic current, it was compared with the experimental data measured at various experimental conditions using RDE apparatus. Figure 6 compares the experimental cathodic current on the surface of steel with the predicted cathodic current at various conditions. The anodic reaction was not taken into account in the model, so there is a deviation between the predicted and measured values around the open circuit potential. This aids in analysis as the pure charge transfer cathodic Tafel can be seen in the modeled curves. Figure 6 shows the model successfully predicted the limiting current values as well as the charge transfer current for both hydrogen and water reduction reactions at various pH and rotational speeds. However, at pH 5, the limiting current is very low and cannot be clearly defined in experimental results. Overall, the modeling results agree well with the experimental results.

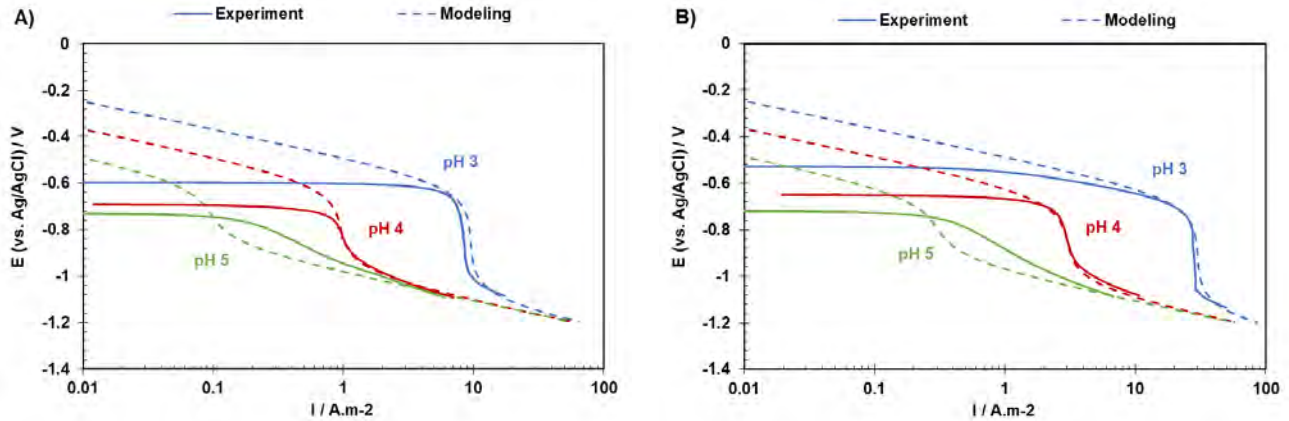


Figure 6. Comparison of experimental and predicted cathodic current densities on the surface of steel at pH 3, 4, and 5 for A) 100 rpm, and B) 1000 rpm.

For the case of pyrite, Figure 7 shows the cathodic currents measured by experiments as well as the predicted cathodic current from the model. The model successfully predicted the charge transfer as well as limiting current of hydrogen reduction reaction at various pH and rotational speeds. The current at very high potentials (close to the pyrite reduction) is not important for galvanic corrosion modeling and therefore a limiting-type current with a constant value was chosen based on the experimental results (e.g., vertical line near $I = 0.1 A.m^{-2}$). Overall, the modeling results agree well with the experimental results.

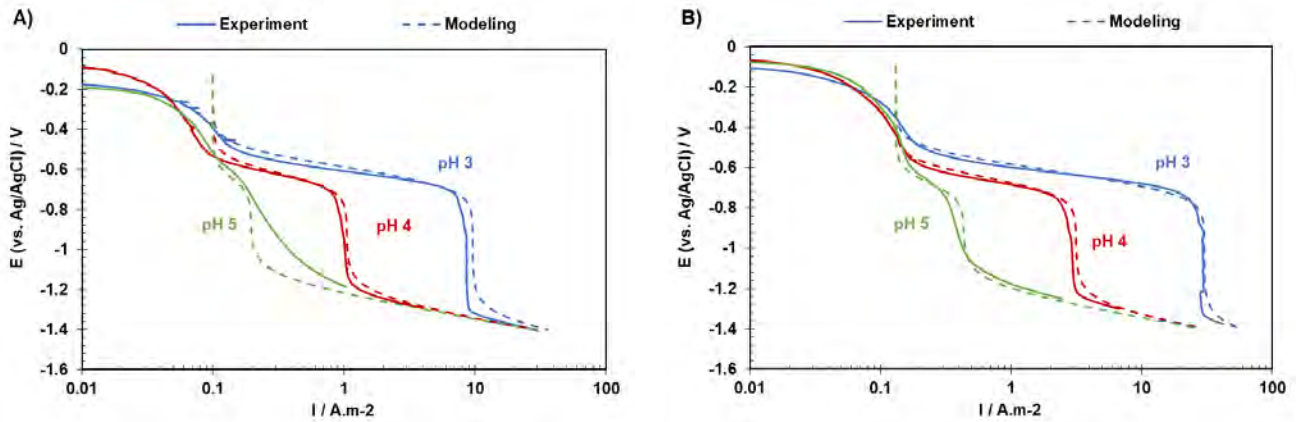


Figure 7. Comparison of experimental and predicted cathodic current densities on the surface of pyrite at pH 3, 4, and 5 for A) 100 rpm, and B) 1000 rpm.

Finally, Figure 8 displays the comparison between experimental and modeled cathodic currents on the surface of pyrrhotite at different conditions. In this case, the high current of the pyrrhotite plays a major role in cathodic current on pyrrhotite surface (vertical line near $I = 4 \text{ A.m}^{-2}$). The H^+ limiting current for cathodic sweeps on pyrrhotite could not be seen at pH 4 and 5 but is visible at pH 3. At pH 3, the model successfully predicts the cathodic behavior. Although the model seems less accurate for pyrrhotite as compared to pyrite, the agreement is still reasonable.

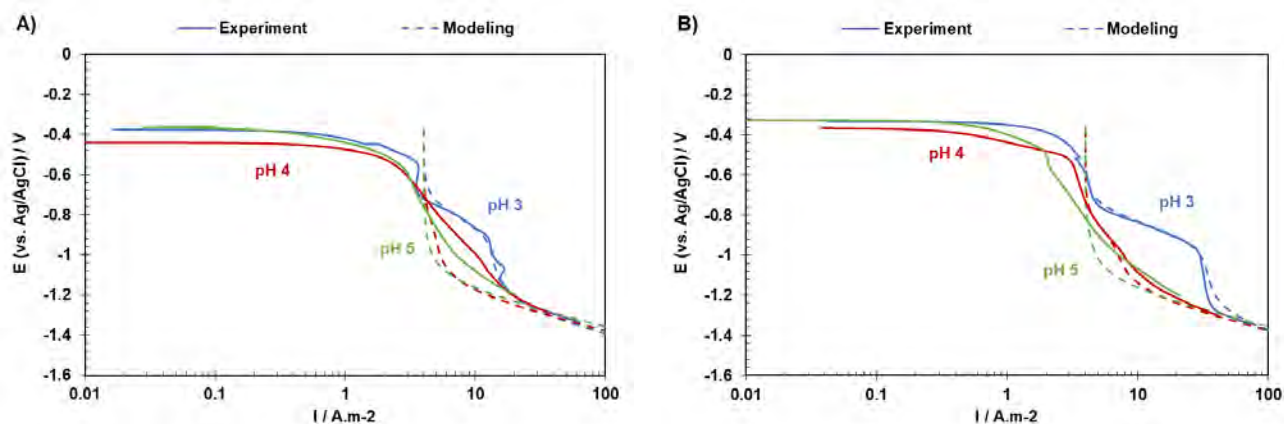


Figure 8. Comparison of experimental and predicted cathodic current densities on the surface of pyrrhotite at pH 3, 4, and 5 for A) 100 rpm, and B) 1000 rpm.

CONCLUSIONS

- Hydrogen reduction as well as water reduction reactions have been verified to occur on pyrite and pyrrhotite surfaces.
- Limiting current for H^+ reduction can be seen on pyrrhotite only at pH 3 as the cathodic current of pyrrhotite is higher than the limiting current of the hydrogen reduction reaction at higher pH values.
- The cathodic current associated with pyrrhotite reduction showed larger current density compared with that associated with pyrite reduction.
- A mathematical model was provided for the cathodic current prediction on the surface of steel and both iron sulfides.
- The model was validated using experimental results. The modeling results agree well with the experimental data.

ACKNOWLEDGEMENTS

The author would like to thank the following companies for their financial support: Ansys, Baker Hughes, Chevron Energy Technology, Clariant Corporation, ConocoPhillips, ExxonMobil, M-I SWACO (Schlumberger), Multi-Chem (Halliburton), Occidental Oil Company, Pertamina, Saudi Aramco, Shell Global Solutions and TotalEnergies.

REFERENCES

1. M. Tjelta, J. Kvarekval, "Electrochemistry of Iron Sulfide and Its Galvanic Coupling to Carbon Steel in Sour Aqueous Solutions", NACE CORROSION/2016; Paper No. 7478.
2. J. Kvarekval, "Morphology of Localized Corrosion Attacks in Sour Environment". NACE CORROSION/2007; Paper No. 7659.

3. J. Ning, "The Role of Iron Sulfide Polymorphism in Localized Corrosion of Mild Steel" Dissertation, Ohio University, 2016.
4. P. Sharifi Abdar, B. Brown, and S. Nescic. "Factors in Galvanic Corrosion between Steel and Iron Sulfides in Acidic Solutions." AMPP Annual Conference + Expo, 2022, San Antonio, Texas, USA
5. S. Navabzadeh Esmaeely, S. Nescic, "Reduction Reactions on Iron Sulfides in Aqueous Acidic Solutions", Journal of Electrochemical Society, 164 C664, 2017
6. P. Sharifi Abdar, M. Bagheri Hariri, A. Kahyarian, S. Nescic, "A revision of mechanistic modeling of mild steel corrosion in H₂S environments", Electrochimica Acta, 382 (2021): 138231
7. A. J. Bard and L. R. Faulkner, Electrochemical Methods: Fundamentals and Applications, John Wiley & Sons, 2002
8. I. C. Hamilton and R. Woods. "An investigation of surface oxidation of pyrite and pyrrhotite by linear potential sweep voltammetry." Journal of Electroanalytical Chemistry and Interfacial Electrochemistry 118 (1981): 327-343
9. Lin, S., Liu, Q. and Li, H., 2014. Electrochemical behavior of pyrite in acidic solution with different concentrations of NaCl. Chinese Journal of Geochemistry, 33(4), pp.374-381.
10. Y. Mikhlin, "Reactivity of pyrrhotite surfaces: an electrochemical study," Phys. Chem. Chem. Phys., 2, 5672 (2000).
11. <https://www.icmt.ohio.edu/web/software/public/freecorp2/>